ChemComm

COMMUNICATION

View Article Online
View Journal | View Issue

Cite this: *Chem. Commun.*, 2024, **60**, 2196

Received 16th September 2023,
Accepted 19th January 2024

DOI: 10.1039/d3cc04199a

rsc.li/chemcomm

The enhanced ionic thermal potential by a polarized electrospun membrane†

Ayesha Sultana, [a] Md. Mehebub Alam, [a] Reverant Crispin [ab] and Dan Zhao *[a]

Inspired by thermally sensitive ion channels in human skin, a polarized membrane composed of a ferroelectric polymer fiber matrix is used to double the heat-induced potential in ionic thermoelectric devices. The comparison of the thermal potentials between different directions of polarization and temperature gradient indicates the importance of cation–dipole interactions for the enhancement.

Ion transport is the most critical physiological process in biological systems because of its key function in regulating the pH value, maintaining osmotic balance and transmitting cellular signals.[1] The principle of sensory perception for living species is directional ion transport across the cell membrane upon external stimuli, which builds up an action potential to be then transported to the brain by nerves to form sensory feedback.[2] The thermal sensation in human skin is performed by a specialized family of membrane proteins containing transient receptor potential (TRP) channels, whose gating is sensitive to temperature.[3] The key function of the membrane is to promote thermally driven ionic charge separation that ultimately results in an electrochemical potential difference.[4] As illustrated in Fig. 1a, the sensory cells are in a resting state with the polarized membrane exhibiting a low potential inside the cells. The external temperature stimuli in Fig. 1b can open the TRP ion channels to induce the influx of cations (sodium ions) into the cells, leading to a rise of membrane potential (so called depolarization process).[5]

The thermal sensing principle in bio-systems has inspired the development of artificial electronic and ionic devices with high sensitivity that can be applied in electronic skin and wearable devices. Pyroelectric and electronic thermoelectric materials have been applied in bio-inspired sensors to directly convert thermal signals into potential changes.[6] Despite the insufficient charge and potential, these concepts only provide electronic charge carriers, which are difficult to integrate with ionic-based bio systems. A gradient polyelectrolyte hydrogel has been demonstrated to have a pressure-sensitive built-in potential analogous to bio-receptors.[7] Nano-fluid membranes were developed to mimic natural thermosensitive and transient receptor potential cation channels.[4,8] However, effectively regulating the thermophoretic mobilities of cations and anions over a wide concentration range of electrolyte solutions remains a challenge.

The thermodiffusion of ions under a temperature gradient could generate a large potential in the scale of millivolts that shares similarity with thermosensitive receptors.[9] This forms the concept of ionic thermoelectrics, which provide an alternative option for thermoelectric materials that is non-toxic and sustainable. The large Seebeck coefficients of ionic thermoelectric

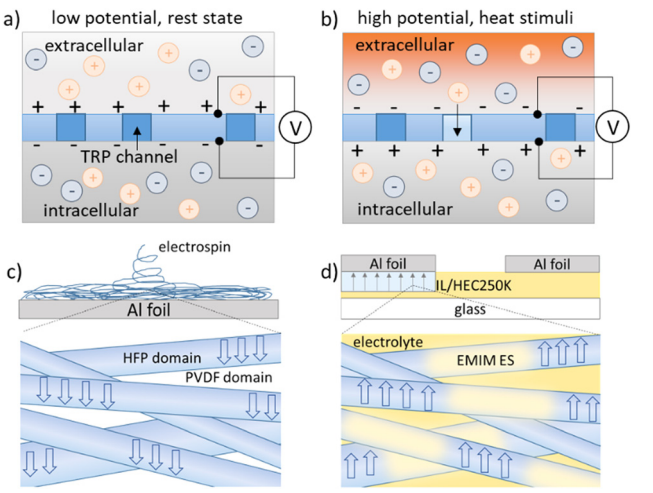

Fig. 1 Diagram depicting the variation of the membrane potential (a) without and (b) with external thermal stimuli. (c) The structure of a polarized membrane composed of electrospun P(VDF-HFP) fiber and (d) an ionic thermoelectric device with the polarized membrane on one electrode.

[a] *Laboratory of Organic Electronics, Department of Science and Technology, Linköping University, Norrköping SE-601 74, Sweden. E-mail: dan.zhao@liu.se*
[b] *Wallenberg Wood Science Center, Linköping University, Norrköping SE-601 74, Sweden*

† Electronic supplementary information (ESI) available. See DOI: https://doi.org/10.1039/d3cc04199a

materials reported in the past ten years also enable the thermal charging of supercapacitors to much higher energy density compared to commercial devices.[10,11] In this work, we investigated the build-up potential of ionic thermoelectric materials across a polarized porous membrane. By comparing the thermally induced potentials with opposite polarization directions and temperature gradients, we discovered that the cation–dipole and cation–polymer interactions are important for the enhancement of the thermal voltage. The optimized polarization could enhance the thermal signal by 2–3 times compared to the only ionic thermoelectric driven response of the same electrolyte. Importantly, different from other reported high ionic Seebeck coefficients between 5 and 26 mV K^{-1}, the large thermal voltage is not affected by encapsulation, which provides a possibility for practical applications with reduced environmental disturbance.

Copolymer poly(vinylidene fluoride-*co*-hexafluoropropylene) P(VDF-HFP) was chosen as the membrane material because it can be polarized with simple treatments (such as electric poling, electrospinning and drawing), and can conduct ions after incorporating an ionic liquid in the HFP amorphous phase.[12–14] As shown in Fig. 1c, electrospinning of P(VDF-HFP) fibers aligns the dipoles inside the crystalline domain (PVDF) vertically to the Al foil collector. This is due to the strong electric field between the needle and the collector of the electrospinning process setup.[15] Experimental details are given in Note S1, ESI.† The characterization of the P(VDF-HFP) polarized membrane is given in Note S2 and Fig. S1, ESI.† The Al foil collectors were cut into strips of 1 mm width to be directly used as electrodes (Fig. 1d). The electrodes contact the ionic liquid electrolytes in a face-down manner to ensure that the electrolytes contact only the membrane-covered surface of the electrodes. 1-Ethyl-3-methylimidazolium ethyl sulfate (EMIM ES) is used here as the ionic thermoelectric material due to the reported high Seebeck coefficient and compatibility with the P(VDF-HFP) membrane.[16] 10 wt% of hydroxyethyl cellulose (HEC) was added into the ionic liquid to improve the stability of the contact without affecting the thermoelectric properties. As shown in Fig. 1b, the ions could pass through the fiber mats, and also dissolve in the amorphous phase of the fibers (HFP domains).[17,18] The ionic conductivity of the electrolyte with and without the P(VDF-HFP) fibermat was characterized by impedance measurements (Note S3 and Fig S2, ESI†). In our previous work, we constructed a fast and sensitive temperature sensor by combining pyroelectric and ionic thermoelectric effects.[19] However, a metal separation layer was used to avoid ion–dipole interactions to simplify the device. Here we truly explored the established potential of ionic thermodiffusion across a polarized membrane of a polymer fiber matrix.

When a temperature difference was applied between the two electrodes, the device functioned as a laterally structured ionic thermoelectric generator (details given in Note S4 and Fig. S3, ESI†). To eliminate the hydrovoltaic effect from water evaporation and absorption when subjected to humidity changes of the atmosphere,[16] the device was encapsulated with polyimide tape (inset of Fig. 2a). Hence, the potential established under heat

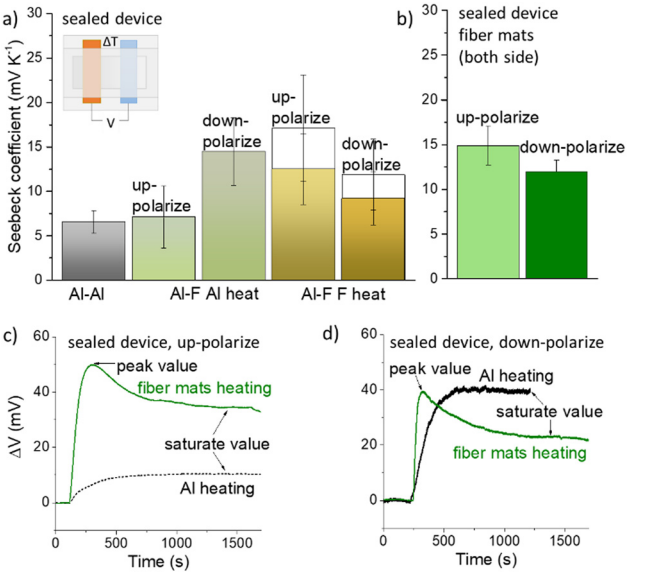

Fig. 2 The Seebeck coefficient of devices with different electrode combinations. (a) The Seebeck coefficient in sealed devices. Inset shows the sealed device structure. (b) The Seebeck coefficient of the devices with a polarized membrane on both electrodes. (c) and (d) The evolution of the thermal voltage under heating for sealed devices. The error bars correspond to the standard deviation from five samples.

stimuli is mostly from the contribution of the ionic thermoelectric effect. The Seebeck coefficient defined as the ratio between the generated thermal potential (saturate value) and the measured temperature difference is presented in Fig. 2a. Details of the measurement setup are presented in Note S4 in the ESI.† Devices with different combinations of electrodes were investigated. The symmetric device with two Al electrodes (Al–Al) can be considered as the control sample, which shows a Seebeck coefficient of around 5 ± 1.3 mV K^{-1} similar to a previous report.[16] With the polarized membrane on the electrode of ionic thermoelectric devices, the dipole-ion interaction and the change of the polarization could affect the established potential under heat stimuli. In order to probe different contributions, we prepared an asymmetric device with one electrode of Al and the other covered by the fibrous polarized membrane (Al–F devices). A temperature gradient was formed by applying a heat stimulus to one electrode while keeping the other one at room temperature. The heat stimuli were first applied on the Al side to induce ionic thermodiffusion in the electrolytes (Al–F Al heat). The polarization strength is expected to not change because the electrode covered by the membrane was kept at constant temperature (RT). This allowed us to investigate the effect of the polarized membrane on the ionic thermodiffusion. As shown in Fig. 2a, the Seebeck coefficient of the devices with an up-polarized membrane (dipole pointing from the electrolyte towards the Al electrode) on the cold side shows a similar value as in an Al–Al device. This indicates that the up-polarized membrane has a minor effect on the ionic thermodiffusion. Surprisingly, the Seebeck coefficient of the devices with the down-polarized membrane on the cold side increased to 15 ± 3 mV K^{-1}. This value is so far among the

highest reported ionic Seebeck coefficients, especially for sealed devices that are not affected by environmental humidity (comparison in Table S1, ESI†). The different impacts of up and down-polarized membranes on the thermal potential indicate that polarization affects the distribution of the ions at the interface of the Al electrodes.

When heat stimuli are applied to the electrodes covered by the membrane (Al–F F heat), the polarization strength will decrease and release the screening charges that are trapped close to the dipoles.[18,19] The results in Fig. 2a show that the Seebeck coefficient of both polarization directions increased. This could be due to the increasing negative charge accumulated on the hot side, or positive charges are forced to diffuse to the cold side. Different from heating Al, a peak appeared at the beginning of the heating and then saturates to a stable voltage (Fig. 2c and d). The peak in the thermal voltage is related to the decreasing of the polarization of the fibrous membrane. The empty columns in Fig. 2a correspond to the data collected form the peak of the thermal voltage.

The differences in the Seebeck coefficients in Fig. 2a show that the polarized membrane could enhance the thermal potential, depending on the direction of the polarization. In Fig. 3, we propose a possible hypothesis that summarizes our experimental observation. For a device with symmetric Al–Al electrodes (Fig. 3a), ionic thermodiffusion induces a thermal voltage when a heat stimulus is applied to one electrode. As shown in Fig. 3a-i and -ii, cations dominate the thermodiffusion to the cold side more than anions and therefore generate a positive potential over the ionic thermoelectric device. By introducing a polarized membrane onto one of the Al electrodes, the ferroelectric dipoles are typically balanced by absorbed screen charge.[20,21] With a heat stimulus applied to the polarized membrane, the polarization decreases and releases a part of the screening charge. This is a complex process because the oppositely charged dipole and screen charge could both affect the electrode potential. Moreover, the P(VDF-HFP) itself could also have an impact on the distribution of the ions due to its strong electronegativity.

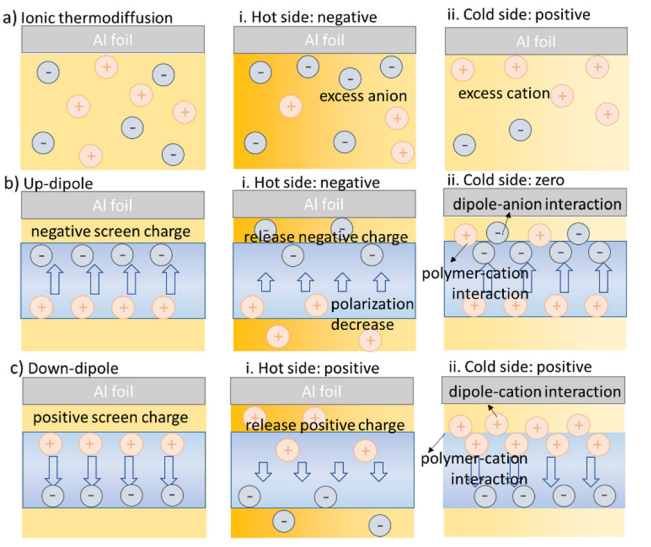

Fig. 3 The illustration of the polarization, ions and their interactions without and with heat stimuli. Three electrodes are presented. (a) Al foil. (b) Al covered with an up-polarized membrane. (c) Al covered with a down-polarized membrane.

Since the thermal voltage increases by heating the membrane with polarization in both directions, we can exclude any major contribution from direct dipole–electrode interactions. This is likely to be the case because the ionic liquid used here could penetrate into the polymer and screen the dipole from interacting with the electrodes. So now we will focus on discussing the distribution of the ions, considering their possible interactions with the dipoles, the polymer chain and the change of the dipoles. First, we investigated the effect of the polarized membrane on the potential of the electrodes. As shown in Fig. S4 (ESI†), the potential of Al covered with polarized fiber mats in both directions is lower compared to the Al electrode. This is due to the strong interaction between the PVDF-HFP and EMIM cation (previously reported),[22] which lead to excess anions at the interface between the membrane and the Al electrode. The FTIR characterizations of the composite in Note S5 (ESI†) indeed imply stronger interactions of the cation-fiber mats compared to the anion-fiber mats. Moreover, the potential of the Al covered with down-polarized fiber mats is higher than the one with up-polarized mats due to opposite dipole–ion interactions. As illustrated in Fig. 3b, the negative side of the dipole could interact with the cation to reach electrostatic equilibrium.[23] The positive side of the dipole interacts oppositely with the anion. However, only the side of the membrane that is adjacent to the electrode could affect the potential of the devices. As shown in Fig. 3b-i, under heating, the up-polarized membrane released anions into the electrolyte that was adjacent to the electrodes, which could contribute to the ionic thermodiffusion, while for the down-polarized membrane, the released cations reduced the effective ionic thermodiffusion (Fig. 2a, Al–F F heat). The potential difference between Al covered by fiber mats with opposite polarization directions under heating (Fig. S7a, ESI†) further suggests the hypothesis of different ion release from the up and down polarized fiber mats.

When the membrane was located on the cold side, the one with down-polarization contributes to the thermal voltage more obviously, according to Fig. 2a (Al–F Al heat). This may be because the negative dipole towards the electrode attracts cations (Fig. 3c-ii). Moreover, as mentioned before, the whole PVDF-based polymer is electronegative due to the strong electron-withdrawing fluorine atoms. Because the polymer hosts cations easier than anions, the effect of the up-polarized membrane in reducing the potential on the cold side is less pronounced (Fig. 3b-ii), although the positive side of the dipole is supposed to interact with the anion. The potential difference between Al covered by different polarized fiber mats as the cold side (Fig. S7b, ESI†) also implies their different abilities of hosting cations. Overall, these interactions lead to the variation of the Seebeck coefficients of the devices in the order of a-i/c-ii > b-i/a-ii > c-i/a-ii > a-i/b-ii > a-i/a-ii. To cross

check this conclusion, we tested the device with symmetric polarized membrane on both electrodes. As shown in Fig. 2b, the Seebeck coefficients of devices with up-polarized membranes is around 15 ± 2 mV K^{-1}. The increase compared to Al being the cold electrode is small and similar to the difference between Al–Al (a-i/a-ii) and Al–F with heating applied to the membrane (a-i/b-ii). This confirms that the up-polarized membrane does not contribute much to the potential on the cold side (Fig. 3b-ii). For the down-polarized membrane, the Seebeck coefficient is lower than a-i/c-ii due to the negative effect of releasing cations on the hot side.

Recent studies on the ionic thermoelectric effect show a major contribution of the hydrovoltaic effect on the resulting thermal voltage in devices with an open surface. Although the energy density depends on the overall thermal voltage,[16] the performance of the device relies largely on the humidity of the atmosphere. Encapsulation of the device could eliminate the environmental dependence and provide better stability for practical applications. From the results shown in Note S6 and Fig S8, ESI,† we discovered that optimized polarization and temperature gradient direction could maintain almost 100% of the thermal voltage with encapsulation. This is an impressive improvement compared to the device without membranes that only shows 60% retention of the potential after encapsulation. We assume that such a function of the membrane could be related to the hydrophobicity of the polymer, the weak dielectric interaction with water and the interaction between the polymer and the cation that bond with water. Further study is needed to better understand the underlying mechanism; we are pleased to discover that the introduction of the polarized membrane could maintain the Seebeck coefficient of 15 ± 3 mV K^{-1} in sealed devices.

To conclude, we build an artificial thermal sensitive receptor with a polarized membrane in an ionic thermoelectric device. The effect of the direction of the polarization and the temperature gradient were investigated to enable us to propose the hypothesis of dipole–ion interaction. The thermal sensitivity of the optimized device increases to double compared to the Seebeck coefficient of the ionic thermoelectric device. Moreover, the potential response to heat stimuli could maintain a high level (Seebeck coefficient =15 ± 3 mV K^{-1}) in a sealed configuration, which provides a new strategy to construct ionic thermoelectric generators.

This work has been financed by the EU commission under the project Metatherm (Project 101058284), as well as the Swedish Research Council (VR 2018-04037), the ÅForsk Foundation (23-220) and the Advanced Functional Materials Center at Linköping University.

Conflicts of interest

There are no conflicts to declare.

Notes and references

1 M. A. Zaydman, J. R. Silva and J. Cui, *Chem. Rev.*, 2012, **112**, 6319–6333.
2 K. A. Hubel and Am. J. Physiol Gastrointest, *Liver Physiol.*, 1985, **248**, G261–G271.
3 T. Voets, G. Droogmans, U. Wissenbach, A. Janssens, V. Flockerzi and B. Nilius, *Nature*, 2004, **430**, 748–754.
4 W. Xian, P. Zhang, C. Zhu, X. Zuo, S. Ma and Q. Sun, *CCS Chem.*, 2021, **3**, 2464–2472.
5 J. Yeom, A. Choe, S. Lim, Y. Lee, S. Na and H. Ko, *Sci. Adv.*, 2020, **6**, eaba5785.
6 W. D. Li, K. Ke, J. Jia, J. H. Pu, X. Zhao, R. Y. Bao, Z. Y. Liu, L. Bai, K. Zhang, M. B. Yang and W. Yang, *Small*, 2022, **18**, 2103734.
7 X. Zhu, P. Qi, W. Fan, H. Wang and K. Sui, *Chem. Eng. J.*, 2022, **438**, 135610.
8 L. Chen, B. Tu, X. Lu, F. Li, L. Jiang, M. Antonietti and K. Xiao, *Nat. Commun.*, 2021, **12**, 4650.
9 D. Zhao, A. Würger and X. Crispin, *J. Energy Chem.*, 2021, **61**, 88–103.
10 D. Zhao, H. Wang, Z. U. Khan, J. C. Chen, R. Gabrielsson, M. P. Jonsson, M. Berggren and X. Crispin, *Energy Environ. Sci.*, 2016, **9**, 1450–1457.
11 B. Kim, J. U. Hwang and E. Kim, *Energy Environ. Sci.*, 2020, **13**, 859–867.
12 A. Sultana, M. M. Alam, S. Fabiano, X. Crispin and D. Zhao, *J. Mater. Chem. A*, 2021, **9**, 22418–22427.
13 P. Martins, A. C. Lopes and S. L. Mendez, *Prog. Polym. Sci.*, 2014, **39**, 683–706.
14 M. M. Alam and X. Crispin, *Nano Res. Energy*, 2023, **2**, e9120076.
15 D. Mandal, S. Yoon and K. J. Kim, *Macromol. Rapid Commun.*, 2011, **32**, 831–837.
16 D. Zhao, A. Sultana, J. Edberg, M. S. Chaharsoughi, M. Elmahmoudy, U. Ail, K. Tybrandt and X. Crispin, *J. Mater. Chem. C*, 2022, **10**, 2732–2741.
17 D. M. Correia, C. M. Costa., S. Serra, J. A. G. Tejedor, L. T. Biosca, V. Z. Bermudez, J. M. S. S. Esperança, P. M. Reis, A. A. Balado, J. M. M. Dueñas, S. L. Méndez and J. L. G. Ribelles, *Polymer*, 2018, **171**, 58–69.
18 C. Xing, M. Zhao, L. Zhao, J. You, X. Cao and Y. Li, *Polym. Chem.*, 2013, **4**, 5726–5734.
19 M. S. Chaharsoughi, D. Zhao, X. Crispin, S. Fabiano and M. P. Jonsson, *Adv. Funct. Mater.*, 2019, **29**, 1900572.
20 A. Sultana, M. M. Alam, T. R. Middya and D. Mandal, *Appl. Energy*, 2018, **221**, 299–307.
21 S. B. Lang, *Phys. Today*, 2005, **58**, 31–36.
22 Z. A. Akbar, Y. T. Malik, D. H. Kim, S. Cho, S. Y. Jang and J. W. Jeon, *Small*, 2022, **18**, 2106937.
23 S. Uchiyama and Y. Katayama, *ACS Omega*, 2022, **7**, 10077–10086.